eHiTS-to-VMD Interface Application. The Search for Tyrosine−tRNA Ligase Inhibitors

Krystian Eitner,*[,†,‡] Tomasz Gawęda,[†] Marcin Hoffmann,*[,†,‡] Mirosława Jura,[†] Leszek Rychlewski,[†] and Jan Barciszewski[§]

BioInfoBank Institute, ul. Limanowskiego 24A, 60-744 Poznan, Poland, Department of Chemistry, Adam Mickiewicz University, Grunwaldzka 6, 60-780 Poznan, Poland, and Institute of Bioorganic Chemistry, Polish Academy of Sciences, Noskowskiego 12, 61-704 Poznan, Poland

Received September 11, 2006

Owing to the recent development of virtual high-throughput screening (vHTS) and a vast number of compounds subjected to vHTS analyses, it has been essential to automate the processing of computational data required for the analysis and visualization of research results. Using the search for tyrosine-tRNA ligase inhibitors as an example, we present a computer application, an interface between eHiTS software for virtual high-throughput screening and VMD graphic software used to visualize calculation results.

INTRODUCTION

The search for ligands that bind strongly to specific proteins has been an arduous and challenging task. High-throughput screening (HTS) is a standard method for the analysis of extensive chemical compound libraries in search of active substances that bind to specific protein receptors.[1,2] That said, HTS is still extremely costly and time-consuming because of the sheer volumes of libraries that contain thousands of potentially biologically active compounds.[3−6] Therefore, there has been a need to apply computational methods so as to screen out at the outset the compounds that, because of their geometric or electrostatic properties, will not effectively bind a specific receptor.

An increase in computer processing power, together with the development of computational methods for protein structure prediction[7−12] and the description of intermolecular interactions,[13−18] has already led to various promising results in drug design.[19−27] In particular, the need to optimize costs and the time required to find compounds with requisite activity has led to the development of varied virtual high-throughput screening methods (vHTS).[4,15,28−30]

Lots of suites and methods are currently available and used to match dock ligands that take into consideration 3D structures of molecules and the chemical match (complementarity) between the receptor and the ligand.[25,31,32] Nevertheless, the majority of tools for ligand docking require considerable processing time especially given the volume of available libraries of potentially biologically active compounds. For example, the Ligand.Info molecule database has more than 1 million chemical compounds.[33,34]

Electronic high-throughput screening (eHiTS) software[14] is a flexible docking tool that systematically fills the space with fragments of a divided inhibitor while ensuring that they do not overlap. A customizable scoring functionality of the eHiTS software has empirical and statistical components and those that factor in local interactions between points of contact of the ligand and the receptor. The software is a practical and comparatively fast method for the docking of ligand molecules to the receptor molecule. It allows for ligand conformational flexibility within reasonable processing time while not taking into consideration receptor conformational flexibility.[14,35,36]

In practice, eHiTS and similar programs generate vast volumes of output data. Output files generated during docking are saved in separate folders for each molecule, which results in a large number of (sub)folders being created. Although the eHiTS vendors provide the CheVi program to visualize eHiTS results,[14] other visualization packages offer additional flexibility. For example, Visual Molecular Dynamics (VMD) is such a program that can be customized to a great extent.[16,37−39] In this case, further processing of the output data stored in hundreds or thousands of folders is necessary.

This paper presents an application that is an interface between the eHiTS docking program and the VMD graphic software. Thanks to the interface, molecules docked to a receptor using eHiTS can easily be visualized in VMD. The operation of the eHiTS-to-VMD application is illustrated by the analysis of results of searching for bacterial tyrosine-tRNA ligase (TyrRS) inhibitors that meanwhile are expected not to bind strongly to human TyrRS.

Aminoacyl-tRNA synthetases (known also as amino acid-tRNA ligases) are interesting objects of study in antibacterial drug design.[40,41] Because of the complementarity between the anticodon sequence built into a respective aminoacyl-tRNA and the coding sequence in mRNA, the information coded in mRNA is translated into amino acid sequences of resulting proteins.[42] Therefore, the synthesis of appropriate aminoacyl-tRNAs, catalyzed by aminoacyl-tRNA synthetases, provides substrates required for protein synthesis. Hence, aminoacyl-tRNA synthetases are essential in the translation of information coded in nucleic acids into protein structures,[43] for they recognize information contained both in the structure of amino acids and in the corresponding tRNA molecules.[44]

* Corresponding author phone: (+48 61) 829 1279 (K.E.); fax: (+48 61) 864 3350 (K.E.); e-mail: eitner@bioinfo.pl (K.E.), mmh@bioinfo.pl (M.H.).
† BioInfoBank Institute.
‡ Adam Mickiewicz University.
§ Polish Academy of Sciences.

10.1021/ci600392r CCC: $37.00
Published on Web 01/18/2007

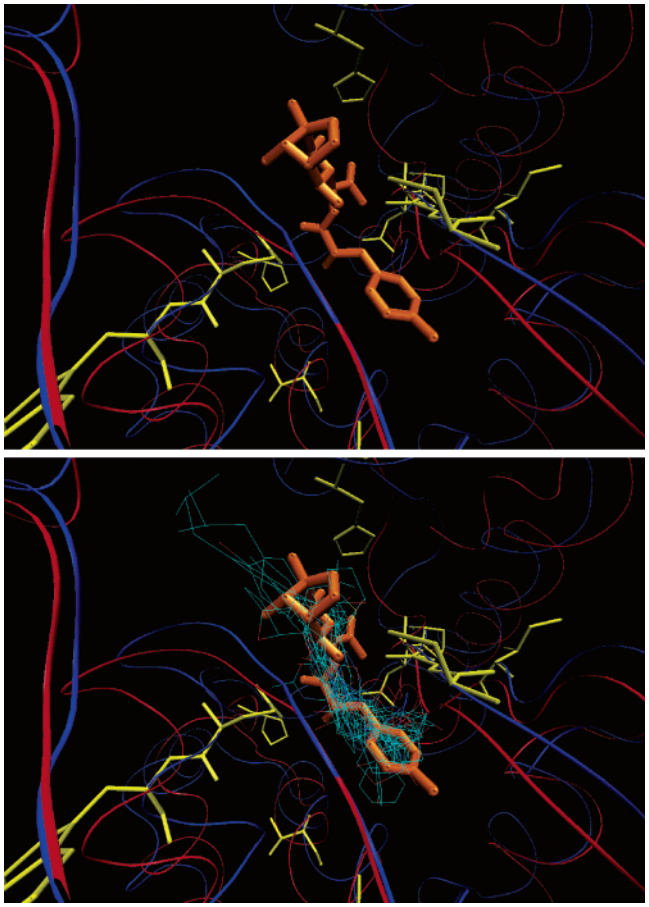

Figure 1. Binding site of tyrosyl-tRNA synthetase from *S. aureus* (red) with the SB-219383 inhibitor (orange) superposed with tyrosyl-tRNA synthetase from *H. sapiens* (blue) depicted in the top panel. The positions of the 10 best inhibitors selected from the set of 340 are presented in the lower panel.

Moreover, studies employing the state-of-the-art methodology of protein structure prediction[45,46] clearly pointed to structural differences between bacterial and mammalian synthetases, making them a promising target in the search for potentially selective bacterial synthetase inhibitors with a low potential for specific interactions with host proteins.[42−44]

Because aminoacyl-tRNA synthetases are instrumental in cell growth and vitality, selective inhibitors of bacterial enzymes (being harmless to humans) will be potent drugs against bacterial infections. Mupirocin,[40] a commercially available antibiotic which inhibits the synthesis of isoleucyl-tRNA, is a good example of such a substance. We decided to select TyrRS for our studies as the Protein Data Bank (PDB) lists the 3D structures of both human[47] and staphylococcal (*Staphylococcus aureus*)[48] enzymes.

Figure 1 shows the structure of an SB-219383 tyrosine-tRNA ligase inhibitor (2S)-2-[[(2S)-2-amino-3-(4-hydroxyphenyl)propanoyl]amino]-2-[(1R,2S,3S,5S,8R)-1,2,4,8-tetrahydroxy-6-oxa-4-azabicyclo[3.2.1]oct-3-yl]acetic acid along with the amino acid residues surrounding the inhibitor at a distance equal to or less than 3.6 Å in the protein from *Staphylococcus aureus* (crystal structure PDB code 1JII). The value of inhibition constant, IC50, for the compound is only 1 nM, making it a very powerful inhibitor of staphylococcal TyrRS,[48] especially in comparison with tyrosinyl adenylate with an IC50 of 11 nM.[48] The bicyclic ring of SB-219383 seen in the crystal structure strongly binds to the staphylococcal protein and occupies the ribose binding site. The hydroxyl group attached to the ring forms a hydrogen bond with Asp195, and His50 forms a hydrogen bond with the molecule fragment adjacent to the bicyclic ring. Furthermore, the bicyclic ring makes hydrophobic van der Waals contacts with Gly38, His50, Pro53, Gly192, and Gly193.[48] Notable is the fact that the active site of the bacterial protein comprises highly conserved amino acid motifs (see Supporting Information Figure S1: alignment between the amino acid sequences of tyrosine-tRNA ligases from selected bacteria and the human enzyme).

Having selected protein target molecules, we still needed a library of molecules to be tested in the vHTS experiment. The library of potential inhibitors for the vHTS experiment was compiled through a literature search[42,43,49] and expanded with the results of searching for similar molecules using the Ligand.Info service. Ligand.Info enables a fast and accurate search for molecules similar to input molecules.[33,34] One of its strongest points is access to a database of more than 1 million commercially available chemical compounds. In general, Ligand.Info's underlying principle is that structurally related molecules display similar behavior upon receptor binding. The database offers interactive clustering of a set of molecules with analogous similarity indices and automatically extracts a set of similar molecules from among the library of over 1 million records. Thus, compounds can be preselected and used both in computational vHTS studies and in wet lab HTS experiments.

COMPUTATIONAL METHODS

Search for Staphylococcal Tyrosine-tRNA Ligase Inhibitors. To illustrate how the eHiTS-to-VMD interface operates, two TyrRS's, human[47] and staphylococcal,[48] have been selected as receptors in the virtual high-throughput screening experiment.

The ligand library was compiled as follows: 34 molecules characterized in the literature[42,43,49] as potential aminoacyl-tRNA synthetase inhibitors were used as a starting point in the search for similar molecules via the Ligand.Info service.[33,34] As a result of the search, the library of potential inhibitors was expanded to a total of 340 molecules used in the virtual high-throughput screening experiment.

The experiment was conducted using eHiTS version 5.3 software:[14] 340 molecules were docked to the human and the staphylococcal TyrRS protein. Enzyme geometries were taken from the Protein Data Bank[50−52] (codes 1N3L and 1JII for *Homo sapiens* and *S. aureus* enzymes, respectively).

In order to speed up vHTS, data on the active site of the 1JII protein were used, which contained the SB-219383 inhibitor {[2-amino-3-(4-hydroxy-phenyl)-propionylamino]-(2,4,5,8-tetrahydroxy-7-oxa-2-aza-bicyclo[3.2.1]oct-3-yl)acetic acid} in the crystallographically characterized structure.

The input parameters for eHiTS were (i) a file with the atomic coordinates of the 1N3L (or 1JII) polypeptide chain (receptor data); (ii) an SDF file with a library of 340 ligands to be docked (ligand data); (iii) a PDB file with the geometry of the TyrRS-inhibitor taken from the protein complex (enzyme active site data). Furthermore, the docking accuracy was set at 6, and SDF was chosen as the output format.

COMPUTATIONAL CONCEPTS

eHiTS-to-VMD Interface. Our application conducts recursive parsing of folders created by eHiTS, divides SDF output files with the geometries of docked molecules into individual files, and arranges them in an order dependent on the value of the scoring function. Subsequently, the application converts the SDF files that eHiTS generated into PDB files, interpretable by most molecule visualization programs. The widely available VMD software was selected for the purpose of our study. It offers a host of useful functionalities with no restriction on the number of opened structure files other than the available RAM.[37]

VMD can be used to visualize and analyze biological systems, such as proteins, nucleic acids, double lipid layers with bound inhibitors, and other small molecules. It may be utilized to visualize any molecule whose structure is available in a format compatible with the PDB[50−52] standard, among others. VMD offers a range of rendering and coloring methods: from straight lines and points to cylindrical structures and advanced ribbon imaging and drawings. Furthermore, the program provides a possibility of creating animations and molecular dynamics imaging based on trajectory analysis. Hence, VMD is a useful tool for the visualization of results of computational experiments, realizable on a computer of choice.[53]

The eHiTS-to-VMD interface presented in this paper generates a VMD script which automatically and quickly visualizes docking results yielded by vHTS experiments. Error-free operation of the eHiTS-to-VMD interface requires that the -out file.sdf option be used when running eHiTS. It should be noted that the -out file.sdf option instructs eHiTS to collect all the best scoring poses into the given file sorted by the score. Moreover, along with eHiTS and VMD, our application uses OpenBabel[54] software to interconvert various formats that code molecule geometries.

The eHiTS-to-VMD application is to be located in a folder created by eHiTS. The default folder where the results generated by eHiTS are saved is $HOME/ehits_work/results/receptor_input_filename/. The OpenBabel software used to convert formats refers by default to folder /usr/bin. eHiTS-to-VMD runs with one of the following options:

- all: This option divides output files, converts files from the SDF to the PDB format, creates a script file for VMD which loads geometries of molecules with the best values of the scoring function, and generates a script file for VMD which loads geometries of 10 molecules with the best values of the scoring function. If the application is used to analyze the docking of a library of molecules to two proteins, the all option will calculate differences between the scoring function values for a given ligand docked to each of the molecules.
- pdb: This option divides output files and converts the output file format from SDF to PDB.
- vmd: This option creates files for two scripts for VMD. One loads geometries of molecules with the best values of the scoring function, and the other creates a VMD script file which loads geometries of 10 molecules with the best values of the scoring function. For this option to run, PDB files have to be created first (manually or automatically through the use of the PDB option).
- clean: This option removes all files generated by eHiTS-to-VMD.
- calc_diff: This option is useful when the interface analyzes the docking of a library of molecules to two proteins. This option calculates differences between the values of the scoring function for the results obtained for both proteins.

Software Requirements. Calculations were performed with eHiTS version 5.3 on a computer cluster built from 28 nodes, running on a Fedora Core distribution of the Linux operation system. For visualization, we used VMD version 1.8.4.[53] The interface application utilized OpenBabel version 1.100.2,[54] gcc version 4.0.3 - The GNU Compiler Collection,[55] glibc6 - GNU C library,[56] and findutil version 1.4.1. The eHiTS-to-VMD interface application was tested on Fedora Core, Debian, and Ubuntu distributions of the Linux operation system.

RESULTS AND DISCUSSION

The calculations conducted using eHiTS yielded 340 folders with output files containing about 30 output geometries for each inhibitor, which totals more than 10 000 files with docked structures of potential inhibitors for each of the enzymes in question.

The main objective of the study was to identify the molecules that bind more strongly to the staphylococcal protein than to the human one. Thanks to the use of the eHiTS-to-VMD interface, molecule geometries with the highest values of the scoring function were found in every folder. Each geometry was subsequently converted to the PDB format. Next, the difference between the scoring function value for a ligand molecule docked in the human and the staphylococcal enzyme was calculated for every ligand. The highest (in absolute value) negative difference denotes an inhibitor with a stronger affinity to the staphylococcal protein than to the human protein; thus, it indicates a potential lead compound for drugs against *S. aureus*.

The differences between scoring function values for the staphylococcal protein and the human protein (differences in $\log K_D$ values calculated with eHiTS) are listed in Table S1 (Supporting Information). The values are in the range of −7.507 (ligand 144) to −1.514 (ligand 171) for the staphylococcal protein and are between −6.203 (ligand 90) and −1.203 (ligand 109) for the human protein. The highest differences in ligand−protein complex dissociation constants were −3.836 (ligand 37, stronger affinity to the staphylococcal protein) and 3.361 (ligand 207, stronger affinity to the human protein).

The position of the SB219383 inhibitor in the human and the staphylococcal TyrRS to which molecules from the library of ligands were docked is shown in Figure 1 (top); the positions of the 20 inhibitors (10 for each protein) characterized by the highest differences in the binding to the staphylococcal and the human protein are shown in Figure 1 (bottom).

Figure 2 shows the chemical structures of 10 molecules with the highest differences in the calculated scoring function values for ligand−human protein and ligand−staphylococcal protein interaction in favor of the bacterial protein complex.

Table 1 lists interactions (distances less than 3.6 Å) between each inhibitor and corresponding residues in the staphylococcal and human proteins according to their structural alignment. The results presented in the table prove

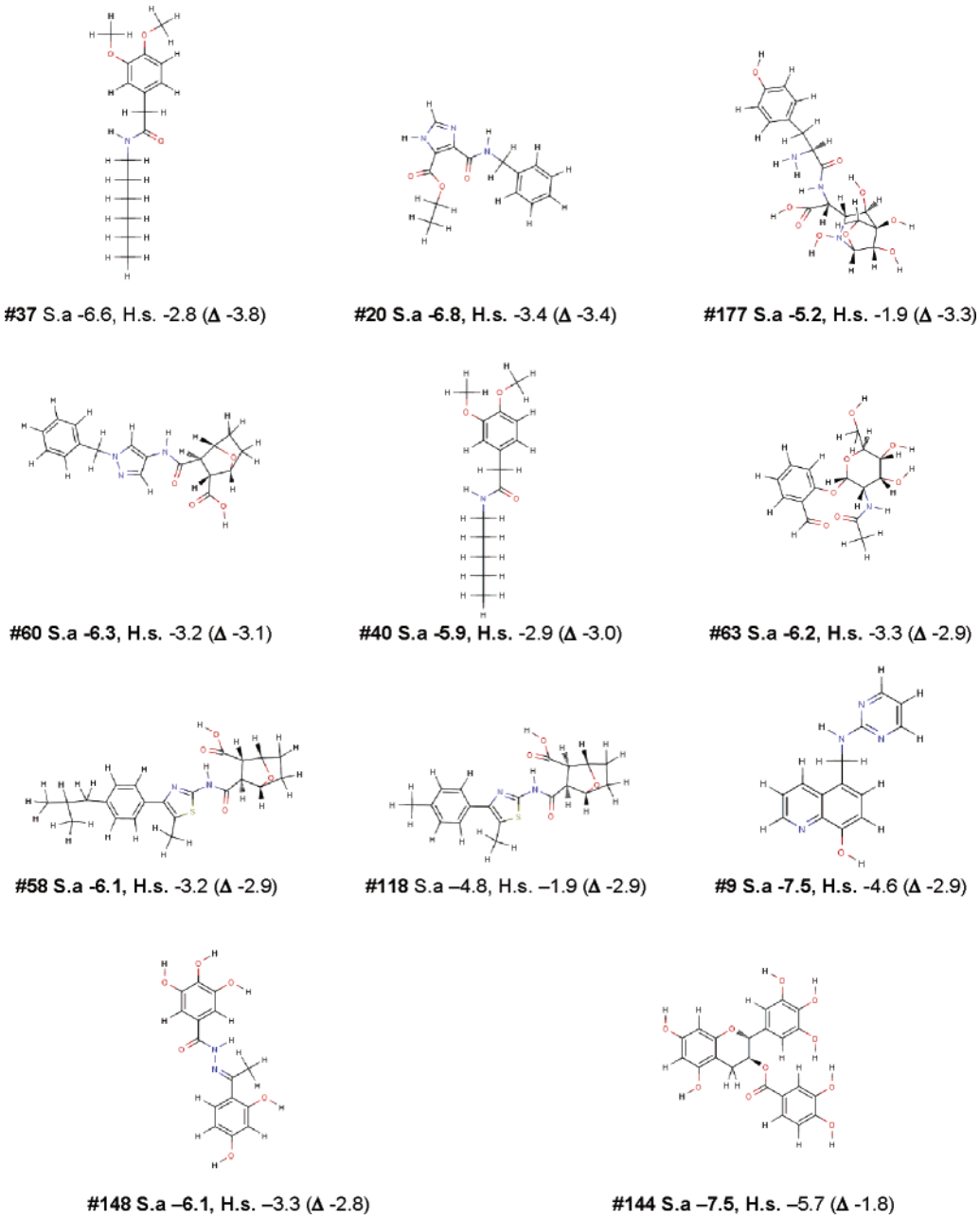

Figure 2. Chemical structure of 10 ligands whose differences in the eHiTS scoring function were the highest in favor of the staphylococcal tyrosyl-tRNA synthetase. The first value (#) is the molecule number; the second value (S.a) is $\log K_D$ calculated with eHiTS for staphylococcal tyrosyl tRNA synthetase; the third value (H.s) is $\log K_D$ calculated with eHiTS for human tyrosyl tRNA synthetase; the fourth value (Δ) is the difference between $\log K_D$'s calculated for staphylococcal and human enzymes.

that inhibitors bind to the active site of the protein and interact with the amino acid residues highly conserved in the sequences of tyrosyl-tRNA bacterial enzymes: Tyr36, Cys37, Gly38, Ala39, Asp40, Thr42, His50, Leu70, Thr75, Asp80, Asn124, Tyr170, Gln174, Asp177, Gln190, Val191, Gly192, Gly193, Asp195, and Gln196 (see Figure 2). However, some of these residues are replaced in the human protein by different amino acids as to their size, shape, and acidity. For example, the acidic Asp40 residue that occurs in the staphylococcal protein is replaced by the smaller and more hydrophobic Ala43 in the human protein. Basic His50 is replaced by fairly similar hydrophilic Tyr52; Asn124, however, is substituted with Gly120, the smallest amino acid. Hydrophobic Leu128 in the *S. aureus* protein is replaced by Gln124 in the *H. sapiens* protein. As for Asp80 in the staphylococcal protein, the corresponding Lys84 residue in the human protein is located beyond the binding site of tyrosyl(adenosine monophosphate) (Tyr-AMP). An optimal overlap of both proteins on the basis of their structural alignment shows the distance between Cα atoms of these residues to be 16.74 Å. Therefore, Asp80 in the *S. aureus* protein cannot be structurally aligned with any residue in the human protein. Notably, a hydrophilic cavity forms in the structure of the bacterial protein between Asp40 and Asp80. By contrast in the human protein, as the aspartate residues are substituted by alanine and the polypeptide chain moves away, the cavity does not form.

These differences in the structure of the active site observed in the bacterial proteins and the human protein show that it may be possible to design an inhibitor that would bind much stronger to the bacterial protein than to the human one.

Table 1. Matrix Presenting Interactions between a Specified Ligand (Top Row) and Amino Acid Residue (Left-Hand Column) for Staphyloccocal (1JII) and for Human (1N3L) Tyrosyl-tRNA Synthetase[a]

1JII/1N3L	37	20	177	60	40	63	58	118	9	148
Tyr36/Tyr39	x/x	x/-	x/-	x/x	x/x	-/-	x/-	x/-	x/-	x/-
Cys37/Trp40	x/x	-/x	x/x	x/x	x/x	-/x	-/x	-/x	x/x	-/x
Gly38/Gly41	x/x	x/x	x/x	x/x	x/x	x/x	x/x	x/x	x/x	x/x
Ala39/Thr42	-/-	x/-	x/x	x/x	x/x	x/x	-/x	x/-	x/x	x/-
Asp40/Ala43	x/x	x/-	x/x	x/x	x/x	x/x	-/x	x/-	-/x	x/-
Thr42/-	-/-	-/-	-/-	-/-	-/-	-/-	-/-	-/-	-/-	x/-
His47/-	-/-	-/-	-/-	-/-	-/-	-/-	-/-	-/-	-/-	x/-
Gly49/Ala51	-/-	-/-	-/-	-/-	-/-	-/-	x/-	-/-	-/-	-/-
His50/Tyr52	x/-	-/-	x/-	x/x	x/-	-/-	-/x	-/-	-/-	x/-
Leu52/Val54	-/-	-/-	-/-	-/-	-/-	-/-	-/x	-/-	-/-	-/-
Pro53/Pro55	-/-	-/-	-/-	x/x	-/-	-/-	x/x	x/-	-/-	-/-
Phe54/Met56	-/-	-/-	-/-	x/-	-/-	-/-	-/-	-/-	-/-	-/-
Leu70/Leu72	-/x	x/x	x/x	x/x	x/x	-/-	x/-	x/x	x/x	x/-
Ile71/Phe73	-/-	-/-	-/-	-/-	-/-	-/-	-/-	x/-	-/-	-/-
Gly72/Ala74	-/x	-/-	x/x	-/x	x/-	-/x	-/-	x/x	-/x	-/x
Thr75/His77	-/x	x/-	x/-	-/-	-/-	x/x	x/x	x/x	x/-	x/x
Asp80/-	-/-	-/-	x/-	-/-	-/-	x/-	-/-	-/-	-/-	-/-
Asn124/Gly120	-/-	x/-	-/-	-/-	-/-	x/-	x/-	x/-	x/-	-/-
Leu159/Val152	-/-	-/-	-/-	-/-	-/-	-/x	-/-	-/-	-/-	-/-
Tyr170/Tyr166	x/x	x/x	x/x	x/-	-/x	x/x	x/x	-/x	x/x	x/x
Leu173/Leu169	-/-	-/-	-/-	-/-	-/-	-/-	-/-	-/-	-/-	-/x
Gln174/Gln170	x/x	-/x	x/x	x/x	-/x	x/-	x/x	-/-	x/x	x/x
Asp177/Asp173	-/x	x/x	x/-	-/-	-/x	x/-	-/-	-/-	-/-	-/x
Gln190/Gln182	x/x	-/x	x/-	x/x	x/x	x/-	x/-	x/-	x/x	-/-
Val191/Phe183	-/x	x/x	-/-	x/x	x/x	x/-	-/-	-/-	-/x	-/x
Gly192/Gly184	-/-	-/x	-/x	-/x	x/x	x/-	-/-	-/x	-/x	-/x
Gly193/Gly185	x/-	-/-	-/x	-/-	x/-	-/-	x/-	x/x	-/-	-/-
Asp195/Asp187	-/-	-/-	x/-	-/-	-/-	-/-	x/-	x/-	-/-	-/-
Gln196/Gln188	x/x	-/x	x/x	x/x	x/x	x/x	-/x	-/x	x/x	-/x
Ile200/Phe192	x/-	-/-	-/-	-/-	-/-	x/-	-/-	-/-	-/-	-/-
Ile221/Asn212	-/-	-/-	-/x	-/-	-/-	-/-	x/-	-/-	-/-	-/-
Pro222/Pro213	-/-	-/-	-/-	-/-	-/-	-/-	x/x	-/-	-/-	-/-
Leu223/Met214	-/-	-/-	-/-	-/-	-/-	-/-	-/x	-/-	-/-	-/-
Val224/Val215	-/-	-/-	-/-	-/-	-/-	-/-	-/x	-/-	-/-	-/-

[a] The x means that the distance between a given ligand and a given amino acid residue was shorter than 3.6 Å. x/x means that the interaction exists with the conserved amino acid residue in both proteins.

Thanks to the use of the eHiTS-to-VMD interface, vHTS calculation results could be visualized very easily. Thus, the differences in the fashion of ligand binding by the human enzyme and bacterial enzymes could be demonstrated to determine why certain ligands bind stronger to the staphylococcal protein.

Ligand 144, a stereoisomer of EGCG isolated from tea[57] (chemical structure shown in Figure 2), is the one with the strongest affinity to the bacterial protein (scoring function value of −7.51). In the bacterial protein, the 3,4,5-trihydroxypheny ring is located near His50 and forms a charge-assisted hydrogen-bond network. The condensed 3,4-dihydro-2H-1-benzopyrane rings are situated in the neighborhood of the tyrosine ring binding site, and the 3,4-dihydroxybenzoic acid ring lies near the ribose binding site. Furthermore, the hydroxyl group at the benzoate ring makes a hydrogen bond with Asp40. The research by Stapleton et al.[58] showed synergic antibacterial activity between antibiotic oxacilline and catechins compounds, such as ligand 144. Zhao et al.[59] explained this synergy by stating that EGCG may bind to peptidoglycan and induce β-lactam susceptibility by interference with cell wall integrity. Our results suggest, however, a different synergy mechanism: By blocking the TyrRS binding site, catechins disrupt bacterial protein synthesis. Thus, the bacteria are weakened and their synthesis of enzymes that catalyze peptide glycan formation is also disrupted, which makes them more susceptible to oxacilline.

In the case of ligand 37, the differences in the calculated scoring function values are the highest in favor of binding the staphylococcal protein (−3.8). The scoring function value for the ligand−staphylococcal protein complex is −6.6, and for the ligand−human protein complex, it is −2.8. The aromatic ring of ligand 37 occupies the tyrosyl residue binding site in the natural Tyr-AMP ligand both in the human and in the staphylococcal protein. However, the arrangement of the methoxy groups in the human protein enables interaction between one of the methoxy groups with Tyr166, whereas in the bacterial protein, the methoxy group makes a contact with Tyr170. In the bacterial protein, the polar portion of ligand 37 (amide bond) is located near polar Cys37.

In the case of ligand 20, the scoring function value is −6.8 for the staphylococcal protein and −3.4 for the human protein. The phenyl group of ligand 20 is located in the ribose binding site for the native Tyr-AMP ligand. In the bacterial protein, the ligand forms a C−H-π interaction with the His50 ring, and the amide group makes a hydrogen bond with the carboxyl group of Asp40. What is more, the imidazole ring interacts with Asp124 via a salt bridge and with Thr75 and Tyr170 via hydrogen bonding. Gln174, positioned above the imidazole ring, interacts with the ester bond of ligand 20. As the ligand is located in an opposite arrangement in the human protein, the phenyl group occupies the tyrosine binding site.

Ligand 177 is the same as the inhibitor in the crystal structure of the staphylococcal TyrRS (1JII). The scoring function value for the staphylococcal protein is −5.2, and for the human protein, it is −1.9. The fact that the ligand has been found as one of the compounds with the highest differences in affinity to the staphylococcal protein and the human protein indicates that eHiTS is indeed useful in virtual high-throughput screening. It must be noted at this point, however, that the ligand's orientation is different from that observed in the crystal structure. Ligand 177, both in the bacterial and in the human protein, is arranged so that the bicyclic ring occupies the tyrosine binding site in Tyr-AMP. The ring interacts with the bacterial protein (Tyr36 and Gln174) at the ether oxygen and with Asn124 via hydrogen bonds with the hydroxyl group. Bacterial Thr75 forms a hydrogen bond with the carboxyl group of ligand 177. In the human protein, Thr75 is substituted by His77, too distant from the carboxyl group to enable strong interaction. In the bacterial protein, the amine group adjacent to the amide bond interacts with Asp80; in the human protein, there are no residues in the vicinity of the site occupied by Asp80 in the bacterial protein, which prevents any interaction that would stabilize the residue. Similarly, the hydroxyl group at the phenyl ring in the staphylococcal protein interacts with His50; the ring in the human protein is located between the hydrophobic Phe183 and Trp40 rings.

The scoring function value for ligand 60 is −6.3 and −3.2 for the staphylococcal and the human protein, respectively. The bicyclic ring of ligand 60, both in the bacterial and in the human protein, is located in the tyrosine binding site for Tyr-AMP. In the bacterial protein, the ether oxygen of the bicyclic ring interacts with Cys37; the hydroxyl group forms a hydrogen bond with His50 and stabilizes the position of

the ring. The amide group is oriented centrally between three residues, Asp80, Asp195, and Gln174, forming a hydrogen-bond network. The group is located in the phosphate binding site for the native Tyr-AMP ligand. The nitrogen atoms of the pyrazole ring interact with Tyr36 and with the main polypeptide chain at Val191. The phenyl ring occupies the tyrosyl binding site. In the human protein, the phenyl ring is located in the neighborhood of the aromatic rings of Tyr166 and His77.

The scoring function value for ligand 40 is −5.9 for the bacterial protein and −2.9 for the mammalian protein. Ligand 40 is positioned in a similar fashion in the bacterial and the human protein. The dimethoxyphenyl ring occupies the tyrosine binding site for the native ligand, and its hydrophobic chain is located in the ribose binding site. In the bacterial protein, the methoxy groups are positioned between Asp40, Asp124, Thr75, and Tyr170, whereas the corresponding amino acid residues in the human protein are more distant with respect to one another so that the methoxy groups cannot fill the cavity completely. The amide group interacts with Cys37 via the oxygen atom, and with the main polypeptide chain at Val191 (bacterial protein) and Phe183 (human protein). The hydrophobic five-carbon ring is located in a cavity of the bacterial protein formed by Pro53, Phe54, Asp195, His50, and Leu221.

The scoring function value for ligand 63 is −6.2 for the staphylococcal enzyme and −3.3 for the human enzyme. The glucose ring of ligand 63 is located between the ribose molecule and the tyrosyl residue for Tyr-AMP in both proteins. The CH_2OH group attached to the glucose ring forms a hydrogen bond with the NH group of the peptide chain at Asp40 in the bacterial protein, and the carboxylate group of Asp40 forms a charge-assisted hydrogen bond with the ligand's amide group. Moreover, the Asp80 carboxylate group makes contacts with the OH groups of the glucose ring. The aldehyde group bound to the aromatic ring interacts with Asp195, and the ring is surrounded by Tyr36 and Cys37. In the human protein, the ring interacts with the Trp40 aromatic ring.

The scoring function value for ligand 58 is −6.1 for the staphylococcal and −3.2 for the human protein. The bicyclic ring of ligand 58, which in both proteins occupies the tyrosyl residue binding site, forms in the bacterial protein an extensive network of hydrogen bonds originating from interactions with Asp40, Thr75, and Asn124. The bonds are formed through the hydroxyl group and the carbonyl oxygen of the amide bond. In the bacterial protein, the thiazole ring forms a bond with Asp195 and the phenyl ring is surrounded by His50 and Asp195 carbon atoms; it occupies the ribose binding site for Tyr-AMP. The hydrophobic isobutyl chain, in turn, is adjacent to Ile221. In the human protein, the hydrophobic fragment of the ligand occupies a hydrophobic cavity formed by Phe183, Tyr52, and Trp40.

As for ligand 118, the scoring function value for *S. aureus* is −4.8, and for *H. sapiens*, it is −1.9. Ligand 118 is spatially oriented in the bacterial protein in a similar fashion to ligand 58. The tyrosyl residue binding site is occupied by the bicyclic ring which forms a network of hydrogen bonds with Asp40, Thr75, and Asn124. In addition, Asp40 binds to the carbonyl oxygen of the ligand's amide group through its peptide-bond nitrogen. The ether oxygen of the bicyclic ring interacts with Tyr 36 and Cys37. The methylphenyl ring, the ligand's hydrophobic part, is surrounded by Asp195 and Pro53. In the human protein, the ligand is in the opposite arrangement, and the methylphenyl group lies in the tyrosine binding site for the native ligand. What's more, the group is situated in the immediate vicinity of hydrophilic residues, His77 and Gln170, which weakens the ligand's affinity in comparison to that to the bacterial protein.

The scoring function value for ligand 9 is −7.5 for the bacterial and −4.6 for the human protein. The structure of ligand 9 includes a guanine group which strongly interacts with Tyr36, Tyr37, Thr75, and Gln174 in the bacterial protein. In the human protein, the group interacts only with Tyr166, and the hydroxyquinoline ring with Trp40. The ligand's pyrimidine ring is located in the tyrosine binding site in both proteins.

The scoring function value for ligand 148 is −6.1 for the staphylococcal and −3.3 for the human synthetase. In the bacterial protein, the aromatic dihydroxyphenyl ring of ligand 148 is located in the tyrosine binding site for Tyr-AMP. The oxygen atom from the hydroxyl group that overlaps with the tyrosine OH interacts with Tyr36 hydroxyl−hydroxyl hydrogen bonds. The other hydroxyl group forms hydrogen bonds with the Asp40 carboxylate group and the Tyr170 hydroxyl group. The remaining molecule fragment, a gallic acid derivative, is involved in a hydrogen-bond network formed through the interaction of the three hydroxyl groups in His47, His50, and Asp195 with the Asp40 peptide bond. In the human protein, the ligand forms a hydrogen-bond network with Gln188 and Thr42 that make contacts with the gallic acid residue.

CONCLUSIONS

Even though diverse applications are available for scientific purposes, there is an urgent need for software that would handle output data between various applications. In particular, the analysis of huge volumes of data generated in virtual high-throughput screening experiments and their visualization remains a largely unsolved issue. Our paper presents a small application, an interface between the eHiTS docking software and the VMD biochemical visualization tool. The eHiTS-to-VMD interface helps analyses and visualizations of large amounts of data generated in vHTS experiments. Thanks to our application, the processing of the extensive body of data yielded in the virtual high-throughput screening experiment was automated and a group of 10 potential inhibitors with a stronger affinity to the staphylococcal tyrosine-tRNA ligase than to the human protein were selected within a comparatively short time. What is more, the visualization of the computational results enabled us to analyze the interactions of the potential TyrRS inhibitors for both proteins we studied. In the course of our studies, we reproduced a much stronger affinity of the SB219383 ligand to the bacterial than to the human enzyme. We were also able to suggest another group of potential inhibitors of bacterial TyrRS. Notably, the compound with the highest scoring function value, and the strongest affinity to the bacterial protein, is a catechol compound, an isomer of ECG isolated from tea. This may indicate that the synergy effect shown between catechins compounds and oxacilline (one of penicillins) originates from the disruption of bacterial protein synthesis by catechins that results from their blocking the TyrRS active site and

disrupting tyrosyl-tRNA synthesis. This type of synergy would be analogous to that observed in penicillins that blocks cell-wall synthesis and aminoglycoside antibiotics that block protein synthesis by binding with bacterial ribosomes.

Important Notice. The eHiTS-to-VMD script described in the paper is freely available from http://eitner.bioinfo.pl/bioinfo/ehits2vmd.sh. Animation presenting the best potential inhibitors in the catalytic pocket of TyrRS and more information about the eHiTS-to-VMD script can be found at http://eitner.bioinfo.pl/bioinfo/ehits2vmd.html.

ACKNOWLEDGMENT

Financial support from European Committee, Grant Nos. BioSapiens LSHG-CT-2003-503265 and GeneFun LSHG-CT-2004-503567, is gratefully acknowledged. Calculations were preformed in the Poznan Supercomputing and Networking Center and Interdisciplinary Computational Center of Adam Mickiewicz University.

Supporting Information Available: SMILES of molecules forming ligand library and calculated values of the score function for interactions with human and staphylococcal TyrRS (Table S1). Multiple alignment of aminoacid sequences of selected tyrosine−tRNA ligases (Figure S1) 1N3L − human protein, (*Staphylococcus aureus* - 1JII) Q2FG09, *Staphylococcus aureus*; Q4L774, *Staphylococcus hemeolyticus*; Q81KS9, *Bacillus anthracis*; Q9A1U3, *Streptococcus pyogenes*; Q97NE3, *Streptococcus pneumoniae*; P0AGJ9, *Escherichia coli*; Q32FD6, *Shigella dysenteriae*; Q8XG70, *Salmonella typhi*; Q9JVY6, *Neisseria meningitidis*; Q5FAF7, *Neisseria gonorrheae*; Q9KUQ0, *Vibrio cholerae*; Q49900, *Mycobacterium leprae*; P67611, *Mycobacterium tuberculosis*; Q6NHG2, *Corynebacterium diphtheriae*; Q6A7W0, *Propionibacterium acnes*; Q9Z8I2, *Chlamydia pneumoniae*; P75122, *Mycoplasma pneumoniae*; P47693, *Mycoplasma genitalium*; Q57DI5, *Brucella abortus*; Q9HWP3, *Pseudomonas aeruginosa*; Q68WH9, *Rickettsia typhi*; O51343, *Borrelia burgdorferi*; P43836, *Haemophilus influenzae*; Q5ZY07, *Legionella pneumophila*; and Q1CT96, *Helicobacter pylori*. A set of 10 figures presenting interactions between human and staphylococcal enzymes and best potential inhibitors. This information is available free of charge via the Internet at http://pubs.acs.org.

REFERENCES AND NOTES

(1) Sills, M. A.; Weiss, D.; Pham, Q.; Schweitzer, R.; Wu, X.; Wu, J. J. Comparison of Assay Technologies for a Tyrosine Kinase Assay Generates Different Results in High Throughput Screening. *J. Biomol. Screening* **2002**, *7*, 191−214.

(2) Klekota, J.; Brauner, E.; Roth, F. P.; Schreiber, S. L. Using High-Throughput Screening Data to Discriminate Compounds with Single-Target Effects from Those with Side Effects. *J. Chem. Inf. Model.* **2006**, *46*, 1549−1562.

(3) Jenkins, J. L.; Kao, R. Y.; Shapiro, R. Virtual Screening to Enrich Hit Lists From High-Throughput Screening: A Case Study on Small-Molecule Inhibitors of Angiogenin. *Proteins* **2003**, *50*, 81−93.

(4) Dorjsuren, D.; Burnette, A.; Gray, G. N.; Chen, X.; Zhu, W.; Roberts, P. E.; Currens, M. J.; Shoemaker, R. H.; Ricciardi, R. P.; Sei, S. Chemical Library Screen for Novel Inhibitors of Kaposi's Sarcoma-Associated Herpesvirus Processive DNA Synthesis. *Antiviral Res.* **2006**, *69*, 9−23.

(5) Smith, S. C.; James, D. R.; Abelman, M. M.; Sexton, G. J. Synthesis and Agrochemical Screening of a Library of Natural Product-Like Bicyclo[2,2,2]octenones. *Comb. Chem. High Throughput Screening* **2005**, *8*, 607−15.

(6) Kogej, T.; Engkvist, O.; Blomberg, N.; Muresan, S. Multifingerprint Based Similarity Searches for Targeted Class Compound Selection. *J. Chem. Inf. Model.* **2006**, *46*, 1201−13.

(7) Ginalski, K.; Elofsson, A.; Fischer, D.; Rychlewski, L. 3D-Jury: A Simple Approach to Improve Protein Structure Predictions. *Bioinformatics* **2003**, *19*, 1015−8.

(8) Ginalski, K.; Grishin, N. V.; Godzik, A.; Rychlewski, L. Practical Lessons from Protein Structure Prediction. *Nucleic Acids Res.* **2005**, *33*, 1874−91.

(9) von Grotthuss, M.; Wyrwicz, L. S.; Pas, J.; Rychlewski, L. Predicting Protein Structures Accurately. *Science* **2004**, *304*, 1597−9.

(10) Plewczynski, D.; Jaroszewski, L.; Godzik, A.; Kloczkowski, A.; Rychlewski, L. Molecular Modeling of Phosphorylation Sites in Proteins Using a Database of Local Structure Segments. *J. Mol. Model.* **2005**, *11*, 431−438.

(11) Kocsor, A.; Kertesz-Farkas, A.; Kajan, L.; Pongor, S. Application of Compression-Based Distance Measures to Protein Sequence Classification: A Methodological Study. *Bioinformatics* **2006**, *22*, 407−412.

(12) Agoston, V.; Cemazar, M.; Kajan, L.; Pongor, S. Graph-Representation of Oxidative Folding Pathways. *BMC Bioinf.* **2005**, *6*, 19.

(13) Zsoldos, Z.; Reid, D.; Simon, A.; Sadjad, S. B.; Johnson, A. P. Ehits: A New Fast, Exhaustive Flexible Ligand Docking System. *J. Mol. Graphics Modell.* **2006**, in press. [doi:10.1016/j.jmgm.2006.06.002].

(14) SimBioSys Inc. http://www.simbiosys.ca/ (accessed Nov 7, 2006).

(15) Yan, S. F.; Asatryan, H.; Li, J.; Zhou, Y. Novel Statistical Approach for Primary High-Throughput Screening Hit Selection. *J. Chem. Inf. Model.* **2005**, *45*, 1784−90.

(16) Amari, S.; Aizawa, M.; Zhang, J.; Fukuzawa, K.; Mochizuki, Y.; Iwasawa, Y.; Nakata, K.; Chuman, H.; Nakano, T. VISCANA: Visualized Cluster Analysis of Protein−Ligand Interaction Based on the *ab Initio* Fragment Molecular Orbital Method for Virtual Ligand Screening. *J. Chem. Inf. Model.* **2006**, *46*, 221−30.

(17) Netzeva, T. I.; Aptula, A. O.; Benfenati, E.; Cronin, M. T.; Gini, G.; Lessigiarska, I.; Maran, U.; Vracko, M.; Schuurmann, G. Description of The Electronic Structure of Organic Chemicals Using Semiempirical and ab Initio Methods for Development of Toxicological QSARs. *J. Chem. Inf. Model.* **2005**, *45*, 106−14.

(18) Hoffmann, M.; Khavrutskii, I. V.; Musaev, D. G.; Morokuma, K. Protein Effects on the O_2 Binding to the Active Site of the Methane Monooxygenase: ONIOM Studies. *Int. J Quantum Chem.* **2004**, *99*, 972−980.

(19) Irwin, J. J.; Shoichet, B. K. ZINC − A Free Database of Commercially Available Compounds for Virtual Screening. *J. Chem. Inf. Model.* **2005**, *45*, 177−82.

(20) Gopalakrishnan, B.; Aparna, V.; Jeevan, J.; Ravi, M.; Desiraju, G. R. A Virtual Screening Approach for Thymidine Monophosphate Kinase Inhibitors as Antitubercular Agents Based on Docking and Pharmacophore Models. *J. Chem. Inf. Model.* **2005**, *45*, 1101−8.

(21) Rella, M.; Rushworth, C. A.; Guy, J. L.; Turner, A. J.; Langer, T.; Jackson, R. M. Structure-Based Pharmacophore Design and Virtual Screening for Novel Angiotensin Converting Enzyme 2 Inhibitors. *J. Chem. Inf. Model.* **2006**, *46*, 708−16.

(22) Pas, J.; von Grotthuss, M.; Wyrwicz, L. S.; Rychlewski, L.; Barciszewski, J. Structure Prediction, Evolution and Ligand Interaction of CHASE Domain. *FEBS Lett.* **2004**, *576*, 287−90.

(23) Pas, J.; Wyszko, E.; Rolle, K.; Rychlewski, L.; Nowak, S.; Zukiel, R.; Barciszewski, J. Analysis of Structure and Function of Tenascin-C. *Int. J. Biochem. Cell. Biol.* **2006**, *38*, 1594−1602.

(24) Schroeder, G.; Wysocka, W.; Łęska, B.; Kolanós, R.; Eitner, K.; Przybylak, J. K. Studies on the Complex Formation Between Lactams and Thiolactams of Sparteine with Copper(II) Cation. *J. Mol. Struct.* **2002**, *616*, 193−199.

(25) Eitner, K.; Bartl, F.; Brzezinski, B.; Schroeder, G. Kinetics of the Protonation of Macrocyclic Amines in the Presence of Monovalent Cations in Aqueous Solution. *Supramol. Chem.* **2001**, *13*, 627−635.

(26) Hoffmann, M.; Chrzanowska, M.; Hermann, T.; Rychlewski, J. Modeling of Purine Derivatives Transport Across Cell Membranes Based on their Partition Coefficient Determination and Quantum Chemical Calculations. *J. Med. Chem.* **2005**, *48*, 4482−4486.

(27) Hoffmann, M.; Rychlewski, J. When, in the Context of Drug Design, Can a Fluorine Atom Successfully Substitute a Hydroxyl Group? *Int. J. Quantum Chem.* **2002**, *89*, 419−427.

(28) Sprous, D. G.; Lowis, D. R.; Leonard, J. M.; Heritage, T.; Burkett, S. N.; Baker, D. S.; Clark, R. D. Optidock: Virtual HTS of Combinatorial Libraries by Efficient Sampling of Binding Modes in Product Space. *J. Comb. Chem.* **2004**, *6*, 530−9.

(29) Plewczynski, D.; Spieser, S. A.; Koch, U. Assessing Different Classification Methods for Virtual Screening. *J. Chem. Inf. Model.* **2006**, *46*, 1098−106.

(30) Liu, Z.; Huang, C.; Fan, K.; Wei, P.; Chen, H.; Liu, S.; Pei, J.; Shi, L.; Li, B.; Yang, K.; Liu, Y.; Lai, L. Virtual Screening of Novel Noncovalent Inhibitors for SARS-CoV 3C-Like Proteinase. *J. Chem. Inf. Model.* **2005**, *45*, 10−17.

(31) Clark, R. D.; Strizhev, A.; Leonard, J. M.; Blake, J. F.; Matthew, J. B. Consensus Scoring For Ligand/Protein Interactions. *J. Mol. Graphics Modell.* **2002**, *20*, 281−95.

(32) Oloff, S.; Zhang, S.; Sukumar, N.; Breneman, C.; Tropsha, A. Chemometric Analysis of Ligand Receptor Complementarity: Iden-

tifying Complementary Ligands Based on Receptor Information (CoLiBRI). *J. Chem. Inf. Model.* **2006**, *46*, 844−51.
(33) von Grotthuss, M.; Koczyk, G.; Pas, J.; Wyrwicz, L. S.; Rychlewski, L. Ligand.Info Small-Molecule Meta-Database. *Comb. Chem. High Throughput Screening* **2004**, *7*, 757−61.
(34) von Grotthuss, M.; Pas, J.; Rychlewski, L. Ligand-Info, Searching for Similar Small Compounds Using Index Profiles. *Bioinformatics* **2003**, *19*, 1041−2.
(35) Chen, H. F.; Dong, X. C.; Zen, B. S.; Gao, K.; Yuan, S. G.; Panaye, A.; Doucet, J. P.; Fan, B. T. Virtual Screening and Rational Drug Design Method Using Structure Generation System Based on 3D-QSAR and Docking. *SAR QSAR Environ. Res.* **2003**, *14*, 251−64.
(36) Gane, P. J.; Dean, P. M. Recent Advances in Structure-Based Rational Drug Design. *Curr. Opin. Struct. Biol.* **2000**, *10*, 401−4.
(37) Humphrey, W.; Dalke, A.; Schulten, K. VMD: Visual Molecular Dynamics. *J. Mol. Graphics* **1996**, *14*, 33−8.
(38) Schwieters, C. D.; Clore, G. M. The VMD-XPLOR Visualization Package for NMR Structure Refinement. *J. Magn. Reson.* **2001**, *149*, 239−44.
(39) Eargle, J.; Wright, D.; Luthey-Schulten, Z. Multiple Alignment of Protein Structures and Sequences for VMD. *Bioinformatics* **2006**, *22*, 504−6.
(40) Ibba, M.; Soll, D. Aminoacyl-tRNA Synthesis. *Annu. Rev. Biochem.* **2000**, *69*, 617−50.
(41) Ibba, M.; Thomann, H. U.; Hong, K. W.; Sherman, J. M.; Weygand-Durasevic, I.; Sever, S.; Stange-Thomann, N.; Praetorius, M.; Soll, D. Substrate Selection by Aminoacyl-tRNA Synthetases. *Nucleic Acids Symp. Ser.* **1995**, *33*, 40−2.
(42) Schimmel, P.; Tao, J.; Hill, J. Aminoacyl tRNA Synthetases as Targets for New Anti-Infectives. *FASEB J.* **1998**, *12*, 1599−609.
(43) Hurdle, J. G.; O'Neill, A. J.; Chopra, I. Prospects for Aminoacyl-tRNA Synthetase Inhibitors as New Antimicrobial Agents. *Antimicrob. Agents Chemother.* **2005**, *49*, 4821−33.
(44) Tao, J.; Schimmel, P. Inhibitors of Aminoacyl-tRNA Synthetases as Novel Anti-Infectives. *Expert Opin. Invest. Drugs* **2000**, *9*, 1767−75.
(45) von Grotthuss, M.; Pas, J.; Wyrwicz, L.; Ginalski, K.; Rychlewski, L. Application of 3D-Jury, GRDB, and Verify3D in Fold Recognition. *Proteins* **2003**, *53 (*Suppl 6), 418−23.
(46) Plewczynski, D.; Pas, J.; von Grotthuss, M.; Rychlewski, L. 3D-Hit: Fast Structural Comparison of Proteins. *Appl. Bioinformatics* **2002**, *1*, 223−5.
(47) Yang, X. L.; Skene, R. J.; Mcree, D. E.; Schimmel, P. Crystal Structure of a Human Aminoacyl-tRNA Synthetase Cytokine. *Proc. Natl. Acad. Sci. U.S.A.* **2002**, *99*, 15369−74.
(48) Qiu, X.; Janson, C. A.; Smith, W. W.; Green, S. M.; Mcdevitt, P.; Johanson, K.; Carter, P.; Hibbs, M.; Lewis, C.; Chalker, A.; Fosberry, A.; Lalonde, J.; Berge, J.; Brown, P.; Houge-Frydrych, C. S.; Jarvest, R. L. Crystal Structure of Staphylococcus Aureus Tyrosyl-tRNA Synthetase in Complex with a Class of Potent and Specific Inhibitors. *Protein Sci.* **2001**, *10*, 2008−16.
(49) Berge, J. M.; Copley, R. C.; Eggleston, D. S.; Hamprecht, D. W.; Jarvest, R. L.; Mensah, L. M.; O'Hanlon, P. J.; Pope, A. J. Inhibitors of Bacterial Tyrosyl-tRNA Synthetase: Synthesis of Four Stereoisomeric Analogues of the Natural Product Sb-219383. *Bioorg. Med. Chem. Lett.* **2000**, *10*, 1811−4.
(50) Bernstein, F. C.; Koetzle, T. F.; Williams, G. J.; Meyer, E. F., Jr.; Brice, M. D.; Rodgers, J. R.; Kennard, O.; Shimanouchi, T.; Tasumi, M. The Protein Data Bank. A Computer-Based Archival File for Macromolecular Structures. *Eur. J. Biochem.* **1977**, *80*, 319−24.
(51) Sussman, J. L.; Lin, D.; Jiang, J.; Manning, N. O.; Prilusky, J.; Ritter, O.; Abola, E. E. Protein Data Bank (PDB): Database of Three-Dimensional Structural Information of Biological Macromolecules *Acta. Crystallogr., Sect. D* **1998**, *54*, 1078−84.
(52) Berman, H. M.; Battistuz, T.; Bhat, T. N.; Bluhm, W. F.; Bourne, P. E.; Burkhardt, K.; Feng, Z.; Gilliland, G. L.; Iype, L.; Jain, S.; Fagan, P.; Marvin, J.; Padilla, D.; Ravichandran, V.; Schneider, B.; Thanki, N.; Weissig, H.; Westbrook, J. D.; Zardecki, C. The Protein Data Bank. *Acta Crystallogr., Sect. D* **2002**, *58*, 899−907.
(53) VMD - Visual Molecular Dynamics. http://www.ks.uiuc.edu/research/vmd/ (accessed Nov 7, 2006).
(54) Open Babel. http://openbabel.sourceforge.net (accessed Nov 7, 2006).
(55) GCC, the GNU Compiler Collection - GNU Project - Free Software Foundation (FSF). http://gcc.gnu.org (accessed Nov 7, 2006).
(56) GNU C Library. http://www.gnu.org/software/libc/libc.html (accessed Nov 7, 2006).
(57) Stammler, G.; Volm, M. Green Tea Catechins (EGCG and EGC) Have Modulating Effects on the Activity of Doxorubicin in Drug-Resistant Cell Lines. *Anticancer Drugs* **1997**, *8*, 265−8.
(58) Stapleton, P. D.; Shah, S.; Hara, Y.; Taylor, P. W. Potentiation of Catechin Gallate-Mediated Sensitization of Staphylococcus Aureus to Oxacillin by Nongalloylated Catechins. *Antimicrob. Agents Chemother.* **2006**, *50*, 752−5.
(59) Zhao, W. H.; Hu, Z. Q.; Okubo, S.; Hara, Y.; Shimamura, T. Mechanism of Synergy Between Epigallocatechin Gallate and Beta-Lactams Against Methicillin-Resistant *Staphylococcus aureus*. *Antimicrob. Agents Chemother.* **2001**, *45*, 1737−42.

CI600392R